Mon. Not. R. astr. Soc. (1986) **220**, 949–969

A cooling flow in the giant, elliptical galaxy NGC 4472

Peter A. Thomas *Institute of Astronomy, Madingley Road, Cambridge CB3 0HA*

Accepted 1986 January 23. Received 1986 January 22; in original form 1985 December 23

Summary. NGC 4472 is shown to contain a large quantity ($10^{10} M_\odot$) of X-ray emitting gas which is cooling and flowing into the centre. The binding of this hot gas in the outer regions of the galaxy requires a substantial halo [$3.5 \pm 0.8 \times 10^{10} (T/10^7\,\mathrm{K})\, M_\odot\,\mathrm{kpc}^{-1}$] of dark matter. We develop a one-phase model for the cooling flow in NGC 4472 and compare this with X-ray surface brightness profiles. We find that (i) the supernova rate must be less than $1.3 \times 10^{-4}\,\mathrm{yr}^{-1}/10^{10}\,L_\odot$ – one twentieth of that given by Tammann; (ii) much of the mass lost from stars via winds or planetary nebulae is confined by the hot phase and rapidly condenses to form new stars; (iii) mass cools out of the hot phase at a rate of $\sim \frac{1}{2}\, M_\odot\,\mathrm{yr}^{-1}$ and does so over the whole galaxy – not just in the central regions. Some of this gas is supplied by an outer reservoir or intragroup medium.

1 Introduction

X-ray emission from normal elliptical galaxies was discovered with the *Einstein* Observatory (Forman *et al.* 1979). Further observations have shown such emission to be common (Long & van Speybroeck 1983; Biermann & Kronberg 1983; Nulsen, Stewart & Fabian 1984; Forman, Jones & Tucker 1985 – hereafter FJT). The X-ray luminosity, L_x, correlates with the optical luminosity, L_o, roughly as $L_x \propto L_o^{1.5-2}$ (Trinchieri & Fabbiano 1985; FJT). The X-ray emission is extended and its spectrum is most consistent with that from a coronal plasma (Nulsen *et al.* 1984; FJT). Although binary X-ray sources are expected to contribute at some level it is most unlikely that they explain the observed high X-ray luminosity in large ellipticals. Observations of the X-ray 'plume' of M86 (Forman *et al.* 1979) and of the diffuse component of Centaurus A (Feigelson *et al.* 1981) argue strongly that hot gas is the dominant source of X-rays.

FJT have recently compiled the X-ray data on 55 early-type galaxies, both elliptical and lenticular. The X-ray emission is well explained by thermal bremsstrahlung and line radiation from a hot gas with $kT \simeq 0.5$–1.5 keV trapped in the galactic potential well. Furthermore the emission lies well above the expected point source flux obtained by extrapolating the $L_x \propto L_o$ relation for fainter galaxies, and in some cases is seen to be reacting to motion through an intracluster medium, thus confirming the gaseous nature of the X-ray emitting material. They deduce that the galaxies must have total masses of at least a few times $10^{12} M_\odot$. The mass of gas in

these systems is substantial ($\simeq 10^{10} M_\odot$) and comparable to that in a large spiral galaxy. Much of this gas may be due to normal stellar mass loss from red giant stars and planetary nebulae, or it could be that remaining from the earliest stages of galactic evolution.

Nulsen *et al.* (1984) showed that the short radiative cooling time of the interstellar gas produced by stellar mass loss within an elliptical would lead to a cooling flow of $\simeq 1 M_\odot \mathrm{yr}^{-1}$. This would explain the X-ray to optical correlation. The cooling gas then condenses back into new stars which are constrained by the colours of early-type galaxies to be of very low mass $M \ll 1 M_\odot$. The arguments in favour of this idea for cooling flows in clusters of galaxies have been given by Fabian, Nulsen & Canizares (1982) and Sarazin & O'Connell (1983). Some of the gas may reach the core of the galaxy and contribute to the visible star formation recently shown to be common (Bertola *et al.* 1980).

The gas may be prevented from forming a cooling flow if it is heated at a rate which exceeds the observed emission. All reasonable heating processes are, however, thermally unstable to cooling (Stewart *et al.* 1984) and so cannot sustain a hydrostatic atmosphere, whilst winds rapidly strip the galaxy of gas and lead to a rate of emission which is much lower than observed.

X-ray studies of early-type galaxies are thus becoming a powerful means for measuring their mass profiles, gas flows and star formation rate. In this paper we analyse in detail the X-ray emission from NGC 4472 – a well-observed giant elliptical in Virgo (from FJT). The time-independent flow equations for interstellar gas in a spherical potential are integrated in Section 2, and the constraints on the structure of the galaxy and its interstellar medium necessary to fit the data are discussed in Section 3. We then compare these results in Section 4 with those of a deprojection method used for clusters of galaxies (Fabian *et al.* 1981). This approach works more directly with the data and gives consistent results. We confirm the necessity for both a massive halo and a cooling flow in NGC 4472. Other well-observed galaxies will be discussed in a subsequent paper.

2 A cooling flow model for elliptical galaxies

We first consider the possibility that the hot gas observed in elliptical galaxies is being ejected in a wind. Time-independent wind solutions have a sonic radius at a few core radii from the centre of the galaxy where mass injection from stellar mass loss still dominates the flow (Mathews & Baker 1971; White & Chevalier 1984), and this condition is confirmed by models with the galactic and halo potentials considered below. At the gas densities inferred from X-ray observations this leads to a rate of escape of gas from the galaxy of 100–$1000 M_\odot \mathrm{yr}^{-1}$, far in excess of the $1 M_\odot \mathrm{yr}^{-1}$ expected from stellar mass loss. (The value for NGC 4472 is evaluated in Section 3.1.) Thus winds, if they exist, must be transient phenomena and so cannot explain the detection of cooling gas in a large fraction of ellipticals. Wind models also have difficulty in fitting the observed surface brightness and temperature profiles since, asymptotically, their density decreases as r^{-2} and their temperature drops to zero. Massive haloes must be very finely tuned in order to slow the rate of escape of gas and produce the correct density decrease without causing the flow to stagnate within the region in which the cooling time is less than a Hubble time. Thus, although some elliptical galaxies may possess winds, those in which hot gas is detected are more likely to contain inflowing material.

In order to model the behaviour of such a system we make the following assumptions:

(i) Fluid properties: The mean time between electron–ion collisions is $10^6 n_{-3}\,\mathrm{yr}$, where the particle number density is $n_{-3} \times 10^{-3}\,\mathrm{cm}^{-3}$. This is much less than the cooling time of the gas (since it must collide in order to cool), but for typical observed densities the mean free path is of order the distance from the centre of the galaxy. The presence of even very weak magnetic fields will

confine the ions to move along field lines, however. These are continually introduced and tangled by stellar mass loss and supernovae so that the effective mean free path is of order the gyration radius. The gas will therefore behave as a simple fluid in local equilibrium.

(ii) Spherical symmetry: This confines the flow to an ever-decreasing volume at the centre and rules out rotational support, but as we are only interested in the solution outside the core these effects are likely to be unimportant. For a discussion of rotation see Cowie, Fabian & Nulsen (1980).

(iii) Time-independence: This requires that the system is evolving only on time-scales longer than the flow time (which is roughly equal to the local cooling time). It will be a good approximation in regions where the flow time is much less than a Hubble time.

(iv) One phase: At any point in the flow, thermal instability ensures that there will be comoving blobs with a range of densities and temperatures (Nulsen 1985). The highest density phases will rapidly condense out, leading to a deposition of cooled gas over a range of radii. We approximate this distribution at each radius by one density and temperature which are characteristic of the gas dynamics. The emission from the bulk of the hot gas is equal to that from a uniform gas at this temperature and density. There is also emission from the rapidly cooling densest phases, the properties of which we take to be those which the mass deposited at that radius would have if it cooled from the characteristic temperature at constant pressure. Note that, in regions where the emission is dominated by the cooling of these densest phases, the characteristic temperature of the observed emission will be about one half of the average temperature of the gas. We assume initially that the mass and energy injection from stellar activity mix uniformly into these phases, so altering only the characteristic density and temperature.

2.1 THE FLOW EQUATIONS

2.1.1 Mass conservation

$$\frac{1}{r^2}\frac{d}{dr}(\varrho u r^2)=\beta-\alpha$$

where r, ϱ, u, β and α are the radius, mass density, inward velocity, mass deposition rate and mass injection rate into the flow respectively.

2.1.2 Momentum conservation

$$\varrho u\frac{du}{dr}-\alpha u=-\varrho\frac{d\phi}{dr}-\frac{dp}{dr}$$

where p is the gas pressure and ϕ the galactic potential. The second term arises because the injected mass is moving relative to the flow

2.1.3 Energy conservation

$$-\varrho u\frac{d\varepsilon}{dr}=\frac{p}{r^2}\frac{d(ur^2)}{dr}+\alpha(\tfrac{1}{2}u^2+\varepsilon_{\rm in}-\varepsilon)-\beta\frac{p}{\varrho}-c$$

where $\varepsilon=\frac{3}{2}(kT/\mu m_H)$ is the specific energy, $\varepsilon_{\rm in}$ is the specific energy of the injected material and c is the cooling function.

The term $\alpha(\frac{1}{2}u^2+\varepsilon_{\rm in}-\varepsilon)$ arises because the injected material has speed u relative to the flow

and is injected with a different energy, and the $-\beta(p/\varrho)$ term arises from the pdV work done on the cooling blobs when they condense out of the flow.

We can rearrange these equations to give

$$\frac{d\log p}{d\log r}=-\text{grav}+\tfrac{5}{3}\,\text{stel}\times\text{Mach}^2-\tfrac{5}{3}\,\text{Mach}^2\frac{d\log u}{d\log r}, \tag{1}$$

$$\frac{d\log \varrho}{d\log r}=\frac{3}{5}\frac{d\log p}{d\log r}-\text{cool}+\text{stel}\left(\tfrac{1}{3}\,\text{Mach}^2+\frac{3}{5}\frac{\varepsilon_{\text{in}}}{\varepsilon}-1\right) \tag{2}$$

and

$$\frac{d\log u}{d\log r}=-2-\frac{d\log \varrho}{d\log r}+\text{stel}\left(\frac{\beta}{\alpha}-1\right) \tag{3}$$

where $\text{grav}=(GM/r)(\mu m_H/kT)$, $\text{stel}=\alpha r/\varrho u$, $\text{Mach}^2=3\varrho u^2/5p$ and $\text{cool}=2n\Lambda r/5\,kTu$ give the relative importance of gravity, mass-injection, velocity and cooling. Here G is the gravitational constant, $M(r)$ is the mass within radius r, μm_H is the mean mass per particle, k is the Boltzmann constant, $T=T_7\times10^7$ K is the gas temperature, n is the number density and $n^2\Lambda$ is the emission per unit volume. These equations can be solved simultaneously for $(d\log p)/(d\log r)$, $(d\log \varrho)/(d\log r)$ and $(d\log u)/(d\log r)$ but, since in practice we find that Mach^2 is out of order 10^{-3} or less, it is a good approximation (with a maximum error of about 1 per cent in p over three orders of magnitude in radius) to replace (1) with the hydrostatic equation

$$\frac{d\log p}{d\log r}=-\text{grav}. \tag{1}'$$

These equations were integrated inwards from a radius of 60 kpc at which the cooling time is of order a Hubble time. Temperatures of T_7 between 1 and 4 to cover uncertainty in the X-ray data, and a density chosen to normalize the count rate, were taken as outer boundary conditions. We then varied the outer velocity to aim for a particular central temperature at 100 pc. The effectively static atmosphere outside 60 kpc, which contributes to the projected emission, was determined by fixing the temperature at the 60-kpc value and using the hydrostatic equation.

2.2 PARAMETERS USED IN THE EQUATIONS

(i) $\mu=0.6$, $\mu m_H=10^{-24}$ g.

(ii) The cooling function is obtained from the code written by Raymond & Smith (1977) using a metal abundance of 0.4 solar as is typical of intracluster gas. Changing this fraction will just result in a change in the normalization of density in the model. The emission is dominated by lines up to temperatures of 3×10^7 K and by bremsstrahlung at higher temperatures.

(iii) The rate of stellar mass loss in early-type galaxies has been estimated by Faber & Gallagher (1976) to be $\alpha=0.015\,M_\odot\,\text{yr}^{-1}/10^9\,L_\odot$.

(iv) The energy injection is dominated by supernovae. Tammann (1974) gives a supernova rate of $2.1\times10^{-3}\,\text{yr}^{-1}/10^{10}\,L_\odot$. For an average Type I supernova of energy 10^{51} erg this gives $6.6\times10^{40}\,\text{erg s}^{-1}/10^{10}\,L_\odot$. There is also the contribution from stellar mass loss which is just $\tfrac{3}{2}\sigma^2\alpha$. It is convenient to write $\varepsilon=\tfrac{3}{2}(kT_{\text{in}}/\mu m_H)$ where $T_{\text{in}}=(\mu m_H/k)\sigma^2+3.4\times10^7$ K.

2.3 COMPARISON WITH WHITE & CHEVALIER (1984)

White & Chevalier (1983 and 1984, hereafter WC) have calculated steady-state solutions in spherical potentials for both wind and infall. In order to check our integration method we used

one of their models as a test case. This has a stellar mass distribution with the analytic approximation to a King (1966) model (hereafter just a King model) of

$$\varrho_* = \varrho_0 \left[1+\left(\frac{r}{a}\right)^2\right]^{-3/2}$$

which is truncated at 200 core radii to keep the total mass finite. The case we consider has a core radius of 500 pc and a total mass of $3.6\times10^{11}\,M_\odot$ corresponding to a central mass density of $46\,M_\odot\,\mathrm{pc}^{-3}$. They used a mass injection rate of $\alpha=6.9\times10^{11}[1+(r/a)^2]$ (corresponding to a mass–luminosity ratio of 10), and $T_{\rm in}=3.56\times10^7$ K. The cooling function of Raymond, Cox & Smith (1976) was used without modification.

The results are given in Fig. 1 and show excellent agreement at all radii. Note that we are forcing the temperature to decrease in the centre, and solutions exist which extend to smaller radii but do not satisfy WC's inner boundary condition.

3 The cooling flow in NGC 4472

NGC 4472 is a giant elliptical galaxy in the Virgo cluster and is the dominant member of the subcluster south of that containing M87 (NGC 4868; Sandage, Binggeli & Tammann 1984; Huchra, Davis & Latham 1984, see also Tanaka 1985). It has been studied extensively at optical wavelengths and has been detected as a very weak radio source (Ekers & Kotanyi 1978; Birkinshaw & Davies 1985). There is no evidence at 21 cm of H I (Huchtmeier, Tammann & Wendker 1975; Kumar & Thonnard 1983) or of optical emission lines (Osterbrock 1960; van den Bergh & Pritchett 1985).

3.1 THE GALACTIC MODEL

The central velocity dispersion was found by Davies (1981) by direct measurement to be $\sigma=260$–$300\,\mathrm{km\,s^{-1}}$ and from Fourier Imaging Techniques to be $\sigma=300$–$340\,\mathrm{km\,s^{-1}}$. This is consistent with Efstathiou, Ellis & Carter (1980) who obtained a line-of-sight velocity dispersion of $306\pm10\,\mathrm{km\,s^{-1}}$ and with Davies *et al.* (1983) who give a literature average of $\sigma=310\pm7\,\mathrm{km\,s^{-1}}$.

Surface photometry by King (1978) gives a core radius of 5.5 arcsec in close agreement with the value of 5.36 arcsec found by Davies (1981). Lauer (1985), however, claims that the previous results are unresolved and gives a deconvolved core radius of 3.7 arcsec. The actual value is not important – we use a value of 5 arcsec which at 20.5 Mpc translates to a core radius of 500 pc. (Note that the results are independent of distance – see later.)

We take the mass profile to follow the luminous profile

$$\varrho_* = \varrho_0 \left[1+\left(\frac{r}{a}\right)^2\right]^{-3/2}.$$

Then $\varrho_0=60\,M_\odot\,\mathrm{pc}^{-3}$ gives a mass of $1.3\times10^{11}\,M_\odot$ within 2.7 kpc in good agreement with Efstathiou *et al.* (1980). Note that this is consistent with the relation of King (1966) for self-gravitating star clusters of

$$\sigma^2=\frac{4\pi G\varrho_0 a^2}{9}\approx(300\,\mathrm{km\,s^{-1}})^2.$$

If the star motions are not isotropic but are more radial, as may be expected if they form from the cooling flow, then the central mass density will be reduced.

The total blue luminosity of NGC 4472, from the *Second Reference Catalogue of Bright*

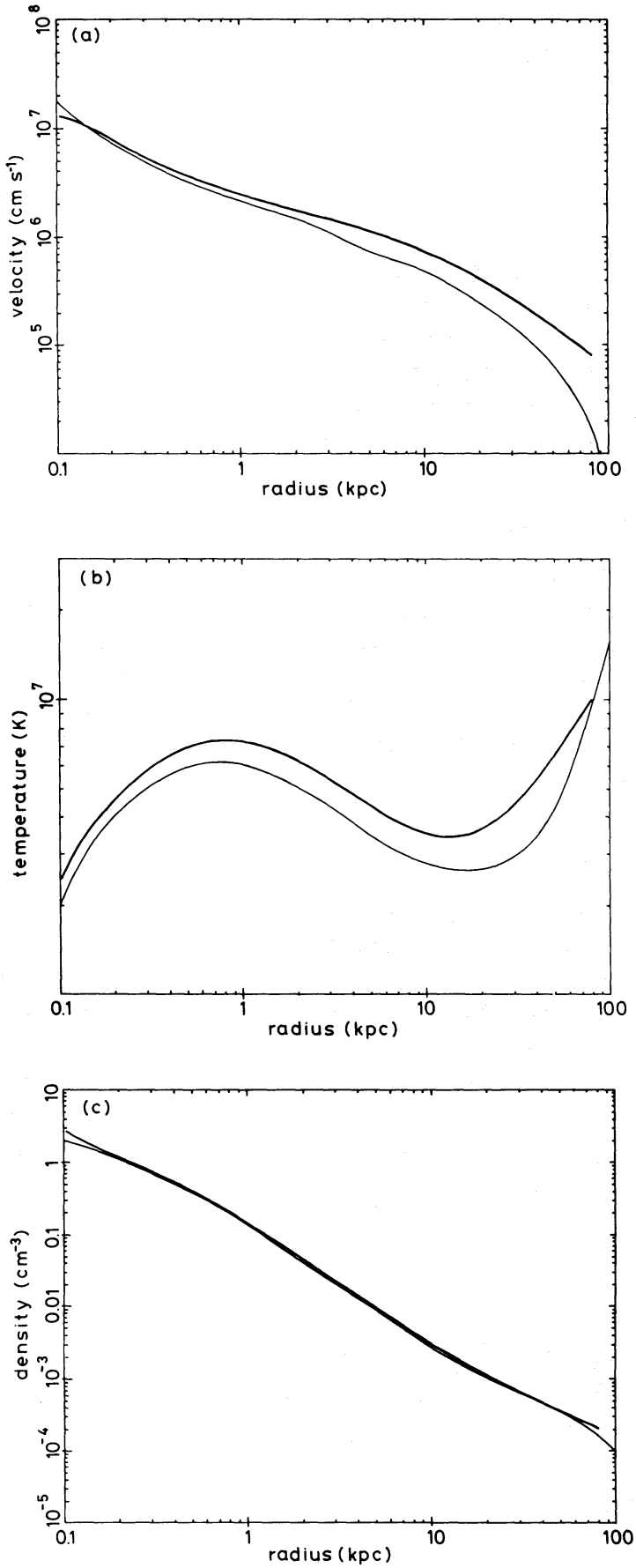

Figure 1. Comparison of our integration method with that of WC. The lower curve extending from 100 kpc in each case is that obtained by WC and these show excellent agreement both in form and in magnitude with our own results.

Galaxies, is $1.5\times10^{11}\,L_\odot$ which gives a luminosity of $7.5\times10^{10}\,L_\odot$ within the de Vaucouleurs effective radius (hereafter just the effective radius) of 10 kpc. This corresponds to a central luminosity density of $L_0\simeq16\,L_\odot\,\mathrm{pc}^{-3}$ so that $\varrho_0/L_0\simeq4$, $\alpha_0=2.4\times10^{10}\,M_\odot\,\mathrm{pc}^{-3}\,\mathrm{yr}^{-1}$ and $T_{\rm in}=4.05\times10^7\,\mathrm{K}$, from a supernova rate of 1/32 yr.

Using the above, we can estimate the mass injection rate needed to sustain a steady wind in NGC 4472. Suppose the flow becomes supersonic within the effective radius (Mathews & Baker 1971, WC). Then mass conservation gives $4\pi a^3\alpha_0\ (\ln 40-1)\simeq4\pi(20a)^2\varrho u$, leading to the condition $\alpha_0>2.2\times10^{-6}\,n(T/10^7\,\mathrm{K})^{1/2}\,M_\odot\,\mathrm{pc}^{-3}\,\mathrm{yr}^{-1}$ which for an observed number density of $0.01\,\mathrm{cm}^{-3}$ (see Fig. 9, later) gives α_0 about 100 times too large.

3.2 COMPARISON WITH THE X-RAY DATA

X-ray surface brightness profiles were obtained by FJT using data from the *Einstein* Observatory Imaging Proportional Counter (IPC) in the energy range 0.5–4.5 keV, and the High Resolution Imager (HRI) in the energy range 0.1–4.5 keV. The centre of the optical and X-ray images agree to within the angular resolution of the HRI (<4 arcsec). The background, from a region >8 arcmin from the galaxy but in the same image, was subtracted from the data, which were then collected into annular bins and converted to surface brightness. Regions containing serendipitous X-ray sources were omitted and spherical symmetry was assumed, although there is some evidence that the X-ray emitting gas is compressed on one side perhaps by motion through an intracluster medium (Fabbiano 1985). The resulting surface brightness profiles are shown in Fig. 2.

The HRI data extend in 10-arcsec bins out to 20 kpc and the IPC data in 24-arcsec bins out to 100 kpc (1 arcsec corresponds to 100 pc at a distance of 20.5 Mpc). The total X-ray luminosity was found to be $3.30\pm0.08\times10^{41}\,\mathrm{erg\,s}^{-1}$, with about half of this originating from within one effective radius. Spectral fitting gives a characteristic temperature of between 0.95 and 1.38 keV within 30 kpc, and a somewhat higher value of 1.25–3.5 keV at larger radii (FJT). This is higher than the virial temperature of $6.5\times10^6\,\mathrm{K}$ deduced from the stellar velocity dispersion.

To compare our model with the data we take the projected emission from hot gas and cooling blobs as described in Section 2, modify by absorption with a galactic column of $1.7\times10^{20}\,\mathrm{cm}^{-2}$ (Stark *et al.*, in preparation) and convolve with the X-ray instrument response to get detector counts. Spatial resolution is important in the IPC and so we also convolve the IPC predicted surface brightness with the impulse response for this characteristic temperature.

3.3 CONSTRAINTS ON THE SUPERNOVA AND MASS INJECTION RATES

The IPC data require that a dark halo be present in order to confine the inferred hot gas. This will be discussed in the next section but will be assumed here. Once the surface brightness beyond 10 kpc is normalized, we find that there is far too much X-ray luminosity produced in the inner regions, with the surface brightness being several times too bright in the central bin [Fig. 3(a)]. In order to get an acceptable fit to the data we have to reduce each of the sources of energy as discussed below.

The energy from supernovae at a rate of $(32\,\mathrm{yr})^{-1}$ estimated above, if effectively deposited into the hot gas, corresponds to a power of $4.1\times10^{41}\,\mathrm{erg\,s}^{-1}$ within an effective radius. Recalling that the X-ray luminosity in this region is only about $1.6\times10^{41}\,\mathrm{erg\,s}^{-1}$, we see that this rate is too high – one supernova per 100 yr is capable of supplying all the observed X-ray power by itself. Our solutions indicate that a rate of at most one supernova per 500 yr is necessary in order to fit the

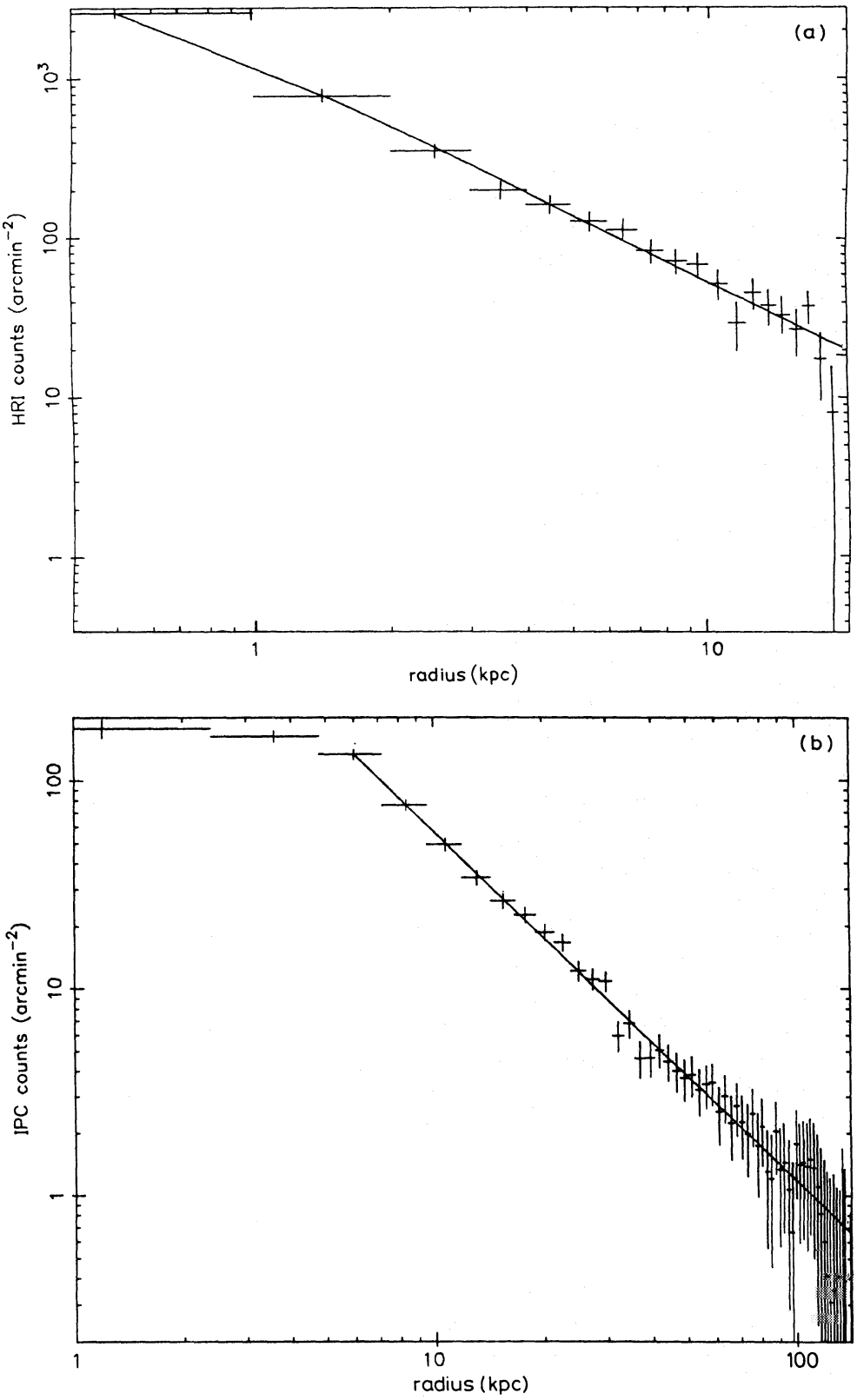

Figure 2. Surface brightness profiles from the *Einstein* High Resolution Imager and Imaging Proportional Counter for NGC 4472 after subtraction of background. The HRI is fitted with an isothermal model

$$\text{const} \times \left[1+\left(\frac{r}{a}\right)^2\right]^{-3\beta+1/2}.$$

The least-squares fit has a core radius of 380 pc and a β of 0.40. The IPC is shown with a power-law fit, excluding the inner two bins, of slope -1.68. The true slope will be less than this since the instrument response tends to steepen the inner regions.

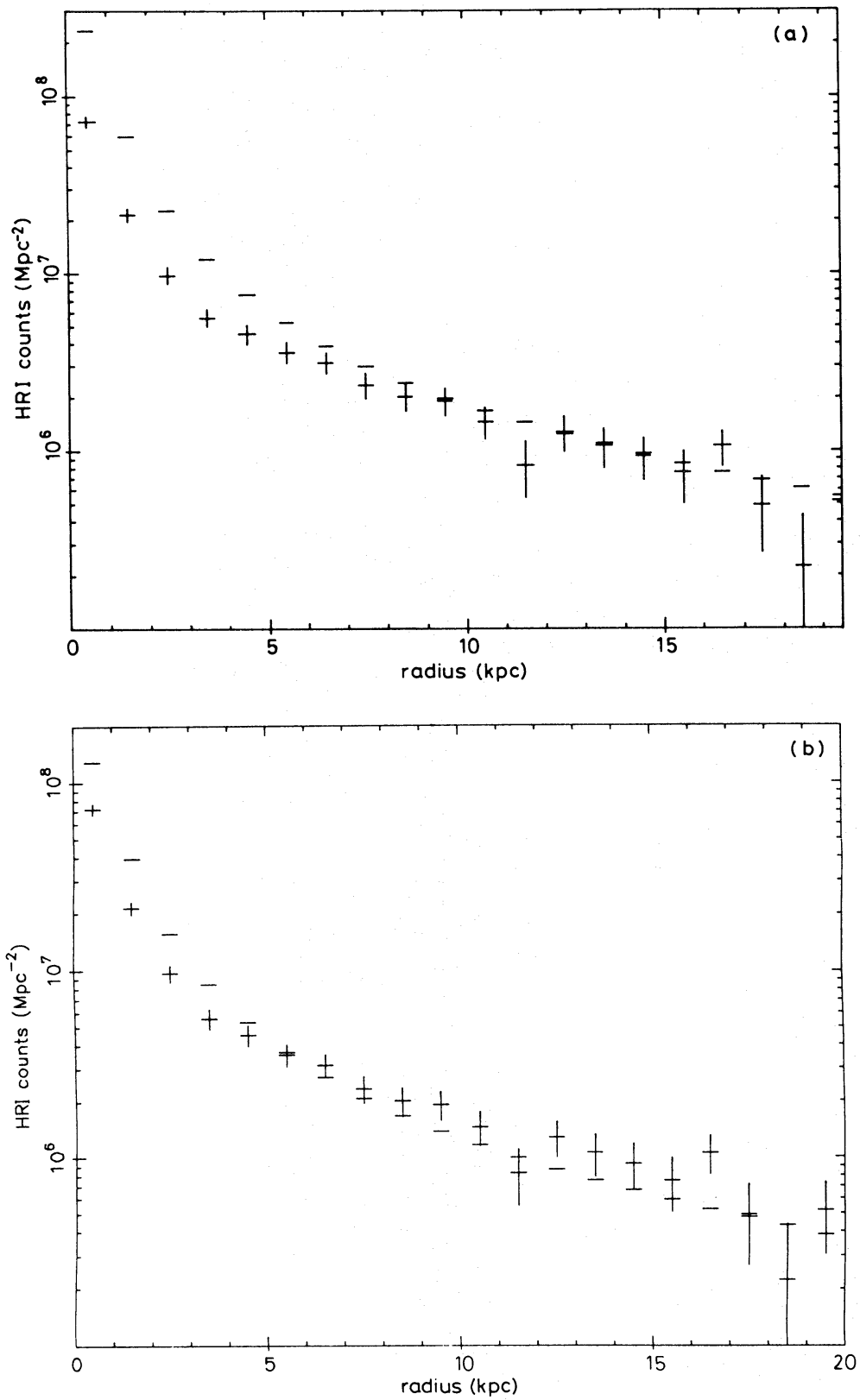

Figure 3. (a) HRI surface brightness profile from our model with supernova energy injection and stellar mass loss rates taken from the literature, and with a constant mass-flow rate. (b) HRI surface brightness profile with supernova energy injection and stellar mass loss reduced to negligible values, and with a constant mass flux over all radii.

data, although this limit can be weakened if a substantial fraction of the kinetic energy of supernovae is radiated below X-ray energies or is otherwise lost. We should stress that the infall solutions are not suppressed by an excess of supernovae but overproduce the X-ray luminosity within the effective radius.

This reduced supernova rate means that the specific energy of the injected material is now close to the virial energy of the stellar motions. At the rate given above, mass injection completely dominates the flow and leads to characteristic temperatures far lower than observed. It also induces cooling of the hot gas already present, leading to mass flow rates of about $1\,M_\odot\,\mathrm{yr}^{-1}$ which once again supply too much energy to the inner regions. To overcome this problem we must consider the details of mass injection by planetary nebulae and red giant winds (see also WC). Most of the stellar mass loss occurs in this way and consists of a localized blob of gas expanding from the central star until its ram pressure is balanced by the thermal pressure of the hot interstellar medium. For a typical planetary nebula of mass $1\,M_\odot$ and temperature $1\text{–}3\times10^4\,\mathrm{K}$, the density will then be $n_\mathrm{b}\simeq10^3\,n_\mathrm{gas}$ and the size $r_\mathrm{b}\simeq0.255\,n_\mathrm{gas}^{-1/3}$ pc. It will be moving relative to the hot gas at the stellar velocity which, at least for NGC 4472, will usually be subsonic with a mean of $v\simeq\sqrt{3}\sigma$. The situation is similar to that of gas being stripped from cluster galaxies by their motion through an intracluster medium as has been discussed by Nulsen (1982). The dominant process will be turbulent, viscous stripping via the Kelvin–Helmholtz instability which tends to break off small blobs of gas from the large one and decelerate them relative to the flow. The rate of breakup and heating of the blobs is very uncertain and depends upon the details of the magnetic fields, although a collision with other dense blobs will certainly cause immediate heating to the virial temperature. The maximum heating rate is of order $\frac{1}{2}\varrho_\mathrm{gas}v^3\Sigma_\mathrm{b}$ where Σ_b is the cross-section, and the rate at which blobs radiate energy is $\Sigma_\mathrm{b}r_\mathrm{b}\Lambda(T_\mathrm{b})$ where r_b is the blob thickness. Thus blobs of size

$$r_\mathrm{b}>\frac{n_\mathrm{gas}}{n_\mathrm{b}}\,\frac{\mu m_H v^3}{2n_\mathrm{b}\Lambda(T_\mathrm{b})},$$

which for $T_\mathrm{b}\simeq1\text{–}3\times10^4\,\mathrm{K}$, $n_\mathrm{b}\simeq1000\,n_\mathrm{gas}$ and $v\simeq520\,\mathrm{km\,s^{-1}}$ is $\simeq0.002\,n_\mathrm{gas}^{-1}$ pc, can easily survive without heating up much above $10^4\,\mathrm{K}$ and will cool and form stars or other objects on a time-scale

$$t_\mathrm{cool}\sim\frac{5kT_\mathrm{b}}{2n_\mathrm{b}\Lambda(T_\mathrm{b})}\sim\frac{R}{v_\mathrm{gas}}\left(\frac{n_\mathrm{gas}}{n_\mathrm{b}}\right)^2\frac{\Lambda(T_\mathrm{gas})}{\Lambda(T_\mathrm{b})}.$$

Here R is the distance from the centre of the galaxy and we have used the fact that the flowtime of the gas is approximately equal to its cooling time. On this time-scale the blob moves a distance $l_\mathrm{cool}=vt_\mathrm{cool}$. The length-scale for being brought to rest relative to the flow is

$$l_\mathrm{stop}\sim\frac{M_\mathrm{b}}{\varrho_\mathrm{gas}\Sigma_\mathrm{b}}=\frac{r_\mathrm{b}n_\mathrm{b}}{n_\mathrm{gas}},$$

where M_b is the mass of the blob, and

$$\frac{l_\mathrm{cool}}{l_\mathrm{stop}}\sim\left(\frac{n_\mathrm{gas}}{n_\mathrm{b}}\right)^3\frac{\Lambda(T_\mathrm{gas})}{\Lambda(T_\mathrm{b})}\,\frac{R}{r_\mathrm{b}}\,\frac{v}{v_\mathrm{gas}}$$

which is very much less than unity except at large radii $R\simeq100$ kpc. Thus, unless the blobs are held at $10^4\,\mathrm{K}$ for many cooling times during the process of star formation, they will rapidly condense out of the flow without being appreciably slowed by it. Blobs which are not significantly heated by motion through the interstellar medium will thus deposit little of their energy into the hot gas.

We now consider the possibility of a collision with other cool blobs which would cause shock

heating to the virial temperature of about 7×10^6 K. The mean free path for collision with other blobs is $\lambda=1/N_b\Sigma_b$ where N_b is the blob number density, so that

$$\frac{l_{stop}}{\lambda}=\frac{M_b N_b}{\varrho_{gas}}$$

which is the mass fraction of cool gas, with l_{cool}/λ being correspondingly smaller. We can place an upper limit on the mass fraction from the non-detection of emission from [O II] λ3727 reported by Osterbrock (1960). He gives an upper limit to the equivalent width of these lines of 1.9 Å which, we estimate, limits the mass fraction in the central regions of cool, dense gas above 1×10^4 K to be less than one quarter of the total gas content. Thus collisions are unlikely to be important and the most important process for transferring mass and energy from the cool blobs to the hot gas is ram-pressure heating. The details are highly uncertain but the above considerations suggest that in the central regions of the galaxy, where $n_{gas}\simeq10^{-1}$ cm^{-3}, the initial blob size is about 30 times larger than necessary to survive heating. Further out, n_{gas} drops to 10^{-3} cm^{-3} and the initial blob size is only a little larger than necessary so that only a small amount of break-up will lead to evaporation. Rather than introduce an arbitrary function of radius to describe the mass-injection rate, we take it to be negligible everywhere. In the following we adopt $\alpha_0=10^{-12}$, corresponding to negligible mass and energy injection from normal stellar activity, and $T_{in}=5.6\times10^8$ K for a supernova rate of 1 per 500 yr. Initially we take the mass deposition by the flow to be zero so that all the cooling gas will reach the centre of the galaxy.

We cannot definitely exclude the possibility that the column density of cooled, cooling and stripped gas provides a significant photoelectric absorption to the emergent X-rays within the inner 10 kpc say. This would reduce the observed value of L_x from the central regions, relaxing the constraints on the energy input from supernovae, and on the mass deposition rate discussed in the next section. Trinchieri (1985) finds, by spectral analysis of the IPC data, that $N_H>3\times10^{20}$ cm^{-2} at 68 per cent confidence i.e. a factor of 2 above the galactic value. This is marginally consistent with the absence of detected cool gas, requiring a mass of about $1\times10^8\,M_\odot$ within 10 kpc. As we explained above, however, the cooling time of X-ray absorbing gas is so short that we do not expect this much to be present. A column of 1.5×10^{20} cm^{-2} provides an absorption of about 10 per cent to 0.5-eV photons and is transparent at energies above about 1 eV.

3.4 CONSTRAINTS ON THE MASS DEPOSITION RATE

If we allow all the inflowing gas to reach the centre of the system, then the gravitational work done on it by the luminous galaxy liberates too much energy and the X-ray surface brightness is still too high in the inner bins by a factor of 2 [Fig. 3(b)]. The potential energy released by a typical flux of $0.6\,M_\odot$ yr^{-1} in falling from infinity to the Galactic Centre is 3×10^{41} erg s^{-1} of which 70 per cent is liberated within 5 kpc. This suggests that the mass drops out of the flow throughout the whole of the galaxy and not just in the core. It is simplest to deposit the cooled gas with the same distribution as the luminous matter and indeed this gives a much better fit to the HRI data, although it is improved by using a core radius of 1 kpc [Fig. 4(a)]. This implies that the luminous stars we observe may have formed from the infalling gas. Dropping the mass out of the flow with the same distribution as the dark matter (see Section 3.5) leads to a surface brightness profile which is too flat [Fig. 4(b)].

3.5 CONSTRAINTS ON THE DARK MATTER

Fig. 5 shows the IPC surface brightness of our model, predicted on the assumption that there is no dark matter in the galaxy and normalized at the centre. Also shown is the total IPC count rate

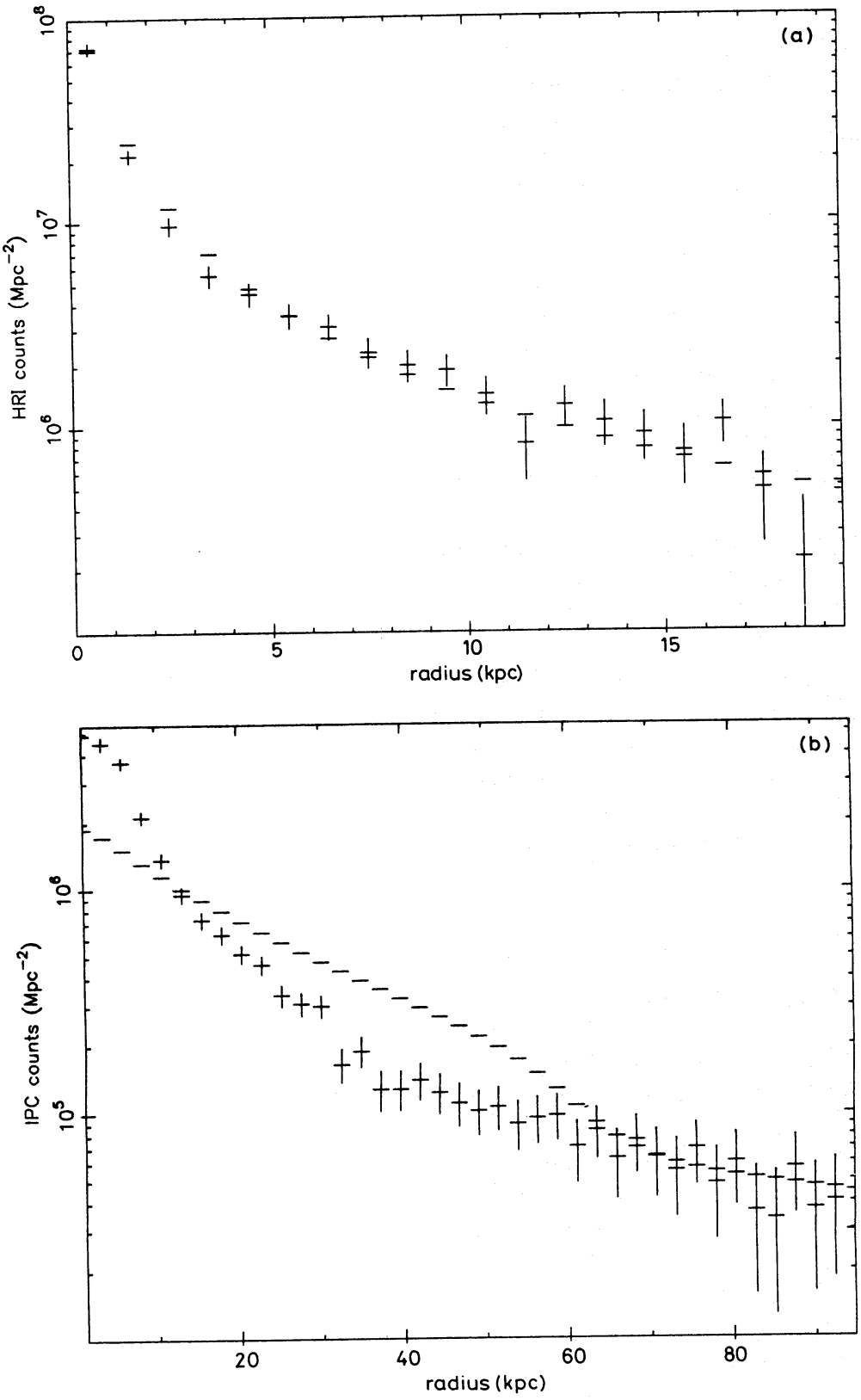

Figure 4. (a) Best-fit model for the HRI surface brightness with mass deposition by the flow as the luminous galaxy is distributed and an outer temperature of 3×10^7 K. (b) Mass deposition as with the dark matter is distributed i.e. with density varying as r^{-2}.

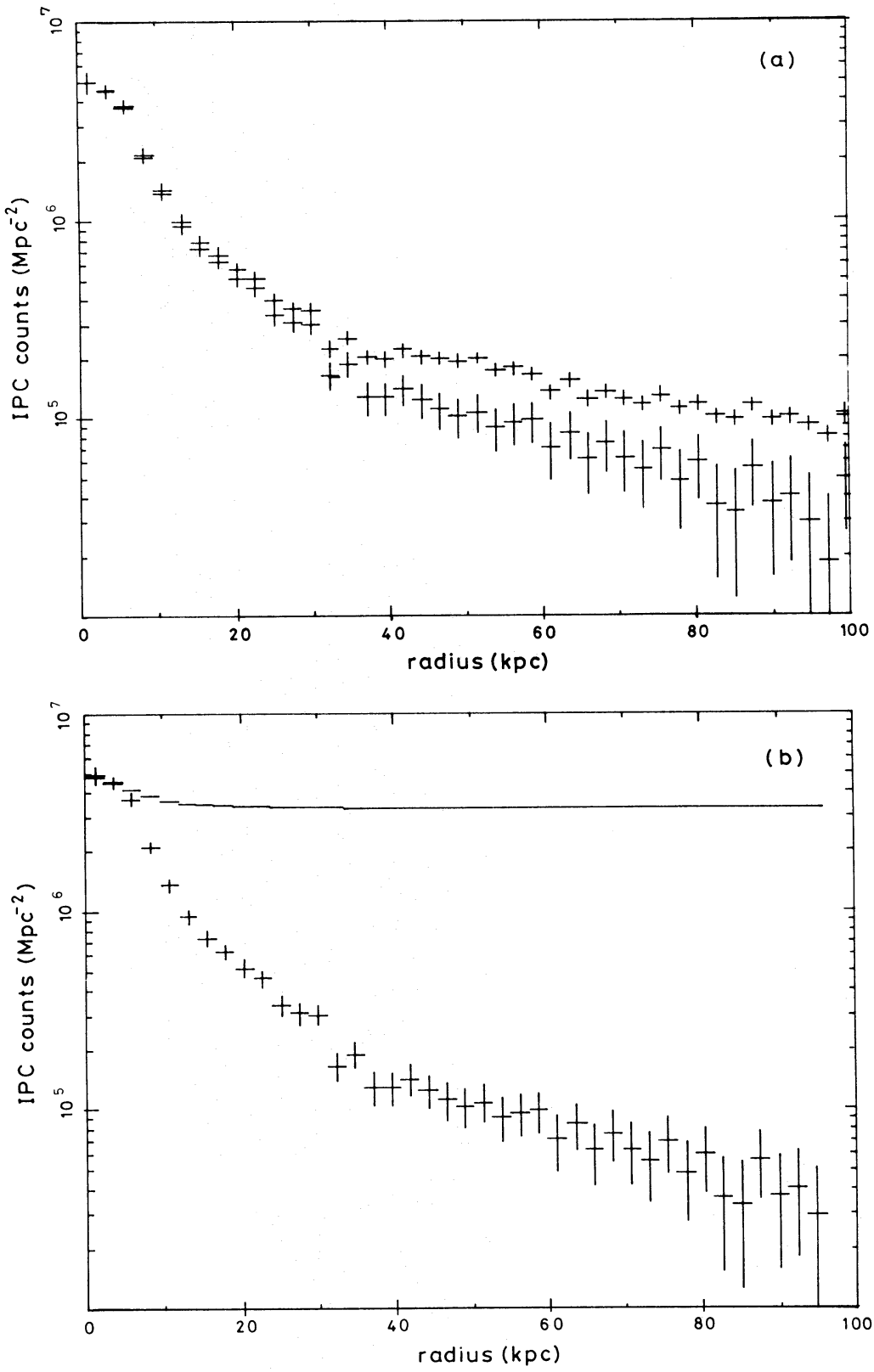

Figure 5. (a) The IPC surface brightness distribution before and after background subtraction. The upper profile limits the amount of gas that can be present even if the background subtraction is too large. (b) The predicted IPC surface brightness from our model with no dark matter present and normalized to be correct in the centre. That an extended atmosphere is not responsible for the gas confinement is shown by Fig. 5(a).

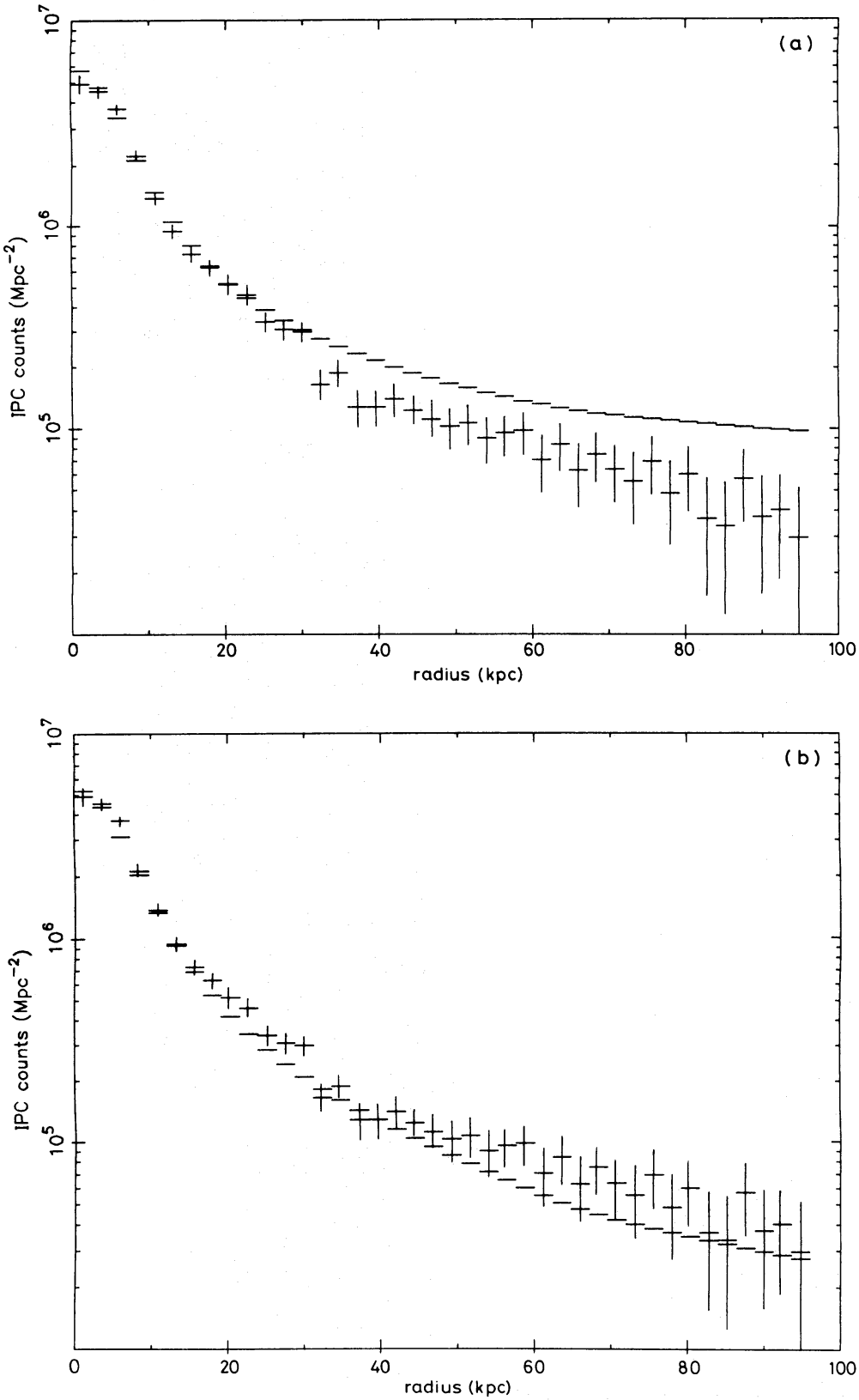

Figure 6. Fits to the IPC surface brightness with a dark halo of (a) $2.7\times10^{10}T_7M_\odot\,\mathrm{kpc}^{-1}$ and (b) $4.3\times10^{10}T_7M_\odot\,\mathrm{kpc}^{-1}$ respectively. Compare with Fig. 5(a) for an estimate of the possible error due to incorrect background subtraction.

before subtraction of the background. It is clear that there is insufficient gravitational potential to bind the observed hot gas even if the background subtraction is too large. The gas is almost in hydrostatic equilibrium with the X-ray surface brightness, varying as $r^{-1.7}$ which for an isothermal gas gives $n \propto r^{-1.35}$. Then from equation (1)′ we have

$$\frac{M(r)}{r} \approx \frac{1.35\,kT}{G\mu m_H} \approx 4.3\times10^{10}\,T_7\,M_\odot\,\mathrm{kpc}^{-1},$$

far in excess of the luminous mass. We therefore added a component of dark mass to our model, taking $\varrho_{\mathrm{dark}}=\varrho_{\mathrm{d}}[1+(r/d)^2]^{-1}$ which gives a constant velocity dispersion at radii greater than the dark-matter core radius d. We found it possible to obtain an excellent fit to the data at radii greater than 10 kpc with a wide range of core radii between 10 and 60 kpc and the total mass of dark matter within 60 kpc normalized to be $2.1\times10^{12}\,M_\odot$ in each case. Smaller core radii can obviously not be excluded although they will increase the gravitational work done on the gas in the inner regions and thus accentuate the problems discussed in previous sections. Fig. 6 shows the IPC fit for a core radius of 10 kpc and a central mass density of $(0.028\pm0.006)T_7\,M_\odot\,\mathrm{pc}^{-3}$, which corresponds to a total mass of $(3.5\pm0.8)T_7\times10^{10}\,M_\odot\,\mathrm{kpc}^{-1}$. This is slightly less than, but consistent with the naïve estimate above. The velocity dispersion is then $\sigma=\sqrt{GM/2r}\simeq275\,T_7^{1/2}\,\mathrm{km\,s}^{-1}$, but, as the measured dispersion out to 10 kpc is dominated by the gravitational potential of the luminous matter, a change in σ would not be observable.

It is possible to put some limits on the error in the required dark mass arising from uncertainties in the model. Any additional sources of X-rays which follow an r^{-2} surface brightness distribution similar to the light, when subtracted from the observed surface brightness, will leave a flatter profile to be explained by the hot gas. These may include the discrete stellar sources which by extrapolation from less luminous galaxies should contribute at the 10 per cent level, and some contribution from the fraction of supernovae energy which does go into heating the hot gas. There should also be some contribution from stellar mass loss which we have assumed to be negligible although, as we explain in Section 3.3, we expect this to be less important in the centre and therefore to have a profile flatter than r^{-2}. Fig. 7 shows the IPC surface brightness profile after subtraction of the largest r^{-2} profile that leaves it non-decreasing all the way into the centre. This corresponds to an energy subtraction of $8\times10^{40}\,\mathrm{erg\,s}^{-1}$. The slope of the residual flux has changed by about 10 per cent and so the potential gradient and therefore the mass per unit radius are uncertain by this amount.

The extent of the dark halo is not well determined, due to uncertainties in the background subtraction and in the temperature profile. FJT give an outer radius of 80 kpc for the X-ray detection, at which point the total mass is $2.8\times10^{12}\,T_7\,M_\odot$ and the pressure is about $2\times10^4\,\mathrm{K\,cm}^{-3}$. If the interstellar gas in NGC 4472 is being compressed by motion through the external medium then this would enable an estimate to be made of the magnitude of pressure confinement. As our data are in circular annuli we cannot comment further on this.

3.6 SUMMARY OF SECTION 3

In summary, we find that it is possible to match the X-ray data with a one-phase cooling-flow model. The overall X-ray luminosity limits the supernova power deposited in the hot gas to be less than that estimated from the supernova rate of Tammann (1974). The detailed shape of the profile requires that mass cools out in a distributed manner so that little gravitational work is performed and that the stellar mass injection rate is less than expected, at least in the central parts of the galaxy. This may plausibly be accounted for by the blobs of injected mass from stellar mass loss recondensing to form stars or other objects without being heated to X-ray temperatures. In this case, much of the mass in the flow originates at the edge of the galaxy and is not due to

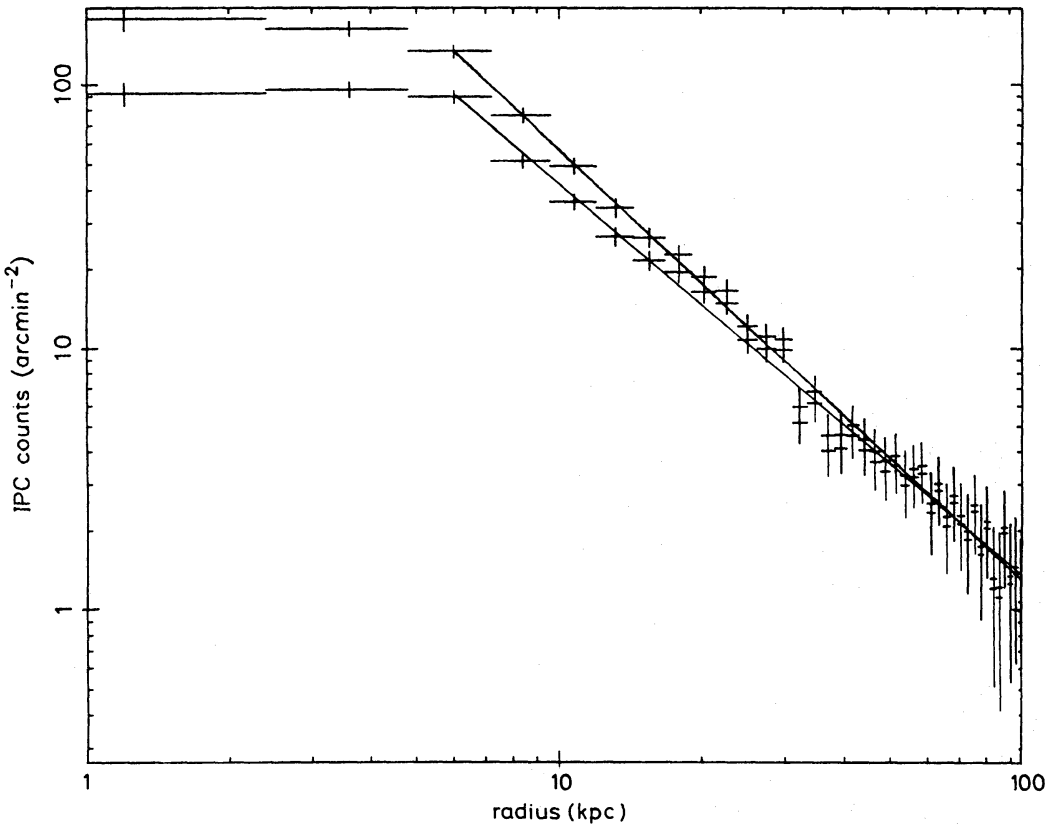

Figure 7. The upper set of points is the original IPC data. The lower set shows the remainder after subtraction of the largest component distributed as the luminous matter that leaves the surface brightness non-decreasing all the way to the centre. The difference in slope between these two profiles indicates the uncertainty in the amount of dark matter present.

(current) stellar mass loss. As NGC 4472 is the dominant member of a subcluster it is likely to be an intermediate case between M87 and NGC 1395, respectively a cluster cooling–flow on to a dominant central galaxy, and flow in an isolated elliptical.

A dark halo is required in order to contain the hot gas. The amount of mass in such a halo is fairly well constrained by the spectral data but its core radius is not well determined. Fig. 8 shows the gas density, temperature and velocity, and the mass-flow rate for our final model.

A realistic multiphase analysis is needed before further understanding can be reached of the gas flows around NGC 4472 and the structure of its interstellar medium. This may prove to be as complex as that in our own Galaxy. We intend to discuss the problem in a later paper.

4 The deprojection method

This is the method described by Fabian *et al.* (1981). An outer pressure, p_{out}, and a gravitational potential for the galaxy are the input parameters needed. The surface brightness data are first deprojected to give count rates per unit volume, by subtracting from each annulus the counts from outer shells projected along the line-of-sight. Then, starting in the outer bin, the temperature needed to produce that count-rate emissivity is estimated by assuming a uniform one-phase medium. The pressure is then increased according to the hydrostatic equation and the procedure repeated for the next shell. If no temperature solution can be found at any stage then a larger value for p_{out} is chosen and the process repeated, starting again at the outer shell.

The deprojection method uses a one-component galaxy model plus a modified King-law potential for the surrounding cluster. We used the latter to mimic the best-fit potential found

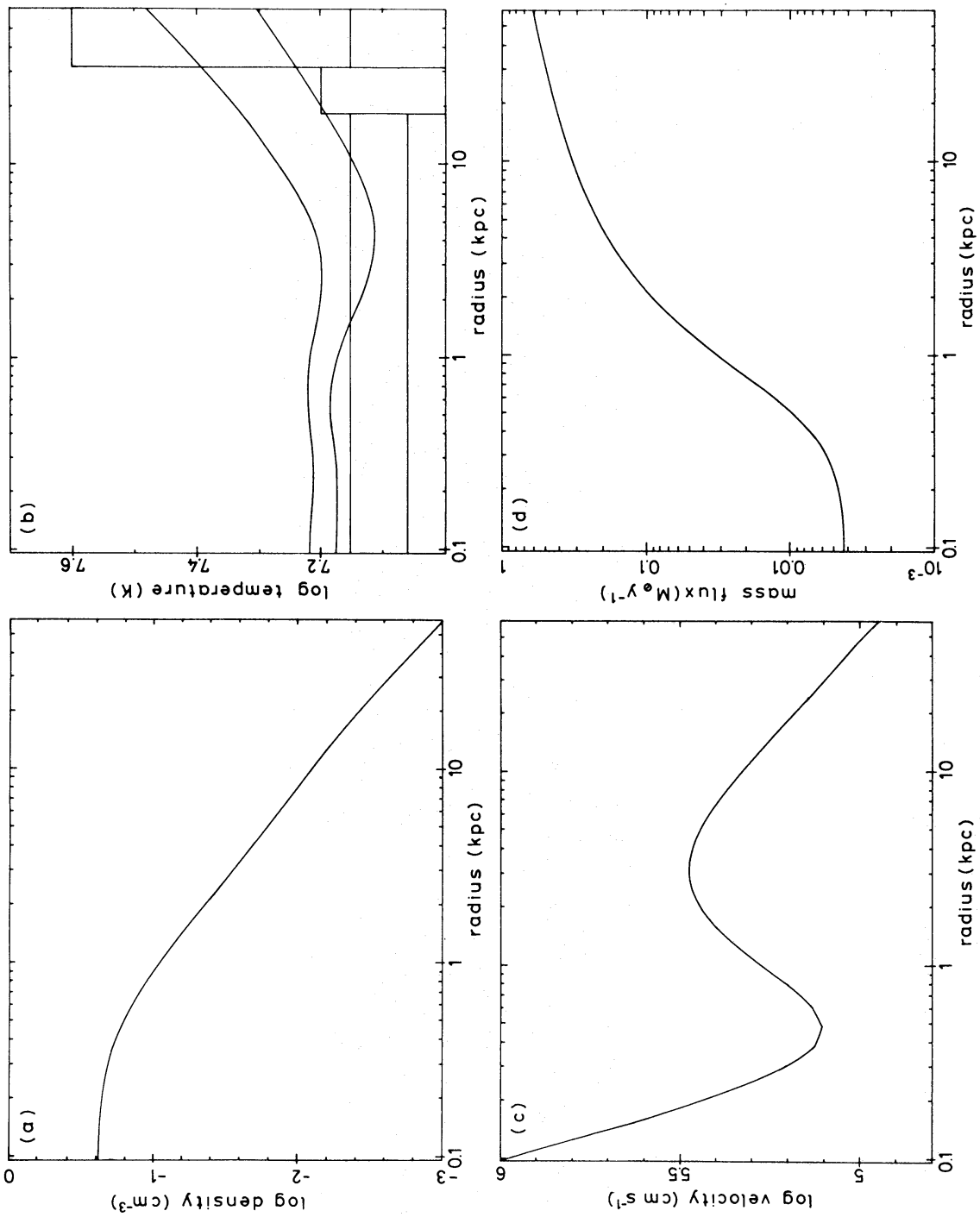

Figure 8. (a) The density profile of our best-fit solution. (b) Temperature profiles for outer temperatures of 3×10^7 and 2×10^7 K. The boxes show the 90-per-cent confidence range of FJT. Note that emission from cooling blobs dominates that from the hot gas phase within about 7 kpc and so the observed temperature is expected to be lower than the model temperature there. The form of the temperature solution within about 1 kpc is fixed by the inner rather than the outer-boundary condition and we have chosen it to be approximately constant. The solution with an outer temperature of 2×10^7 K gives a better fit to the temperature profile but has a worse fit to the HRI data. (c) The velocity profile which is subsonic throughout the whole range. (d) The mass-flow rate.

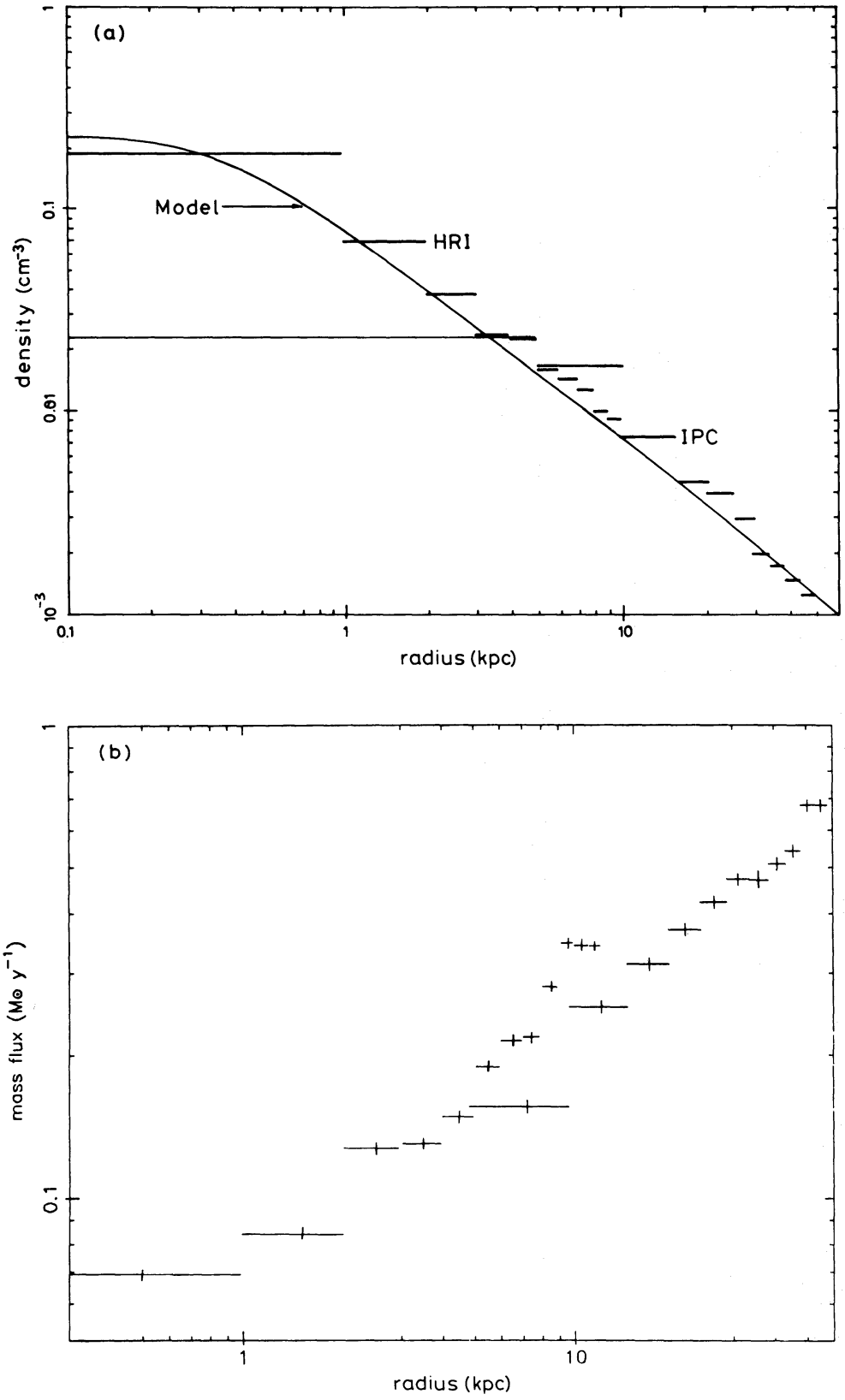

Figure 9. (a) The deprojected density profiles from the HRI and IPC data plotted with that of our model. (b) The deprojected mass flow rates (assuming no mass injection) from the HRI and IPC data.

above for the dark matter. The resultant density profile matched that of our model rather well and is presented for comparison in Fig. 9(a).

The mass-flow rate profile was estimated by assuming that mass injection was negligible and that matter dropped out of the flow uniformly with volume in any one bin. Then

$$\Delta L=\Delta\dot{M}(H+\phi-\langle\phi\rangle_v)_+ +\dot{M}_-\Delta(H+\phi),$$

where subscript + refers to the outer edge of a bin, − to the inner edge of a bin and Δ to the change within a bin. Here L is the luminosity, $\dot{M}$ is the mass flow rate, H is the enthalpy and ϕ is the gravitational potential. We estimate $\langle\phi\rangle_v$ by assuming that the potential is uniform with radius over any one bin. Then

$$\Delta\dot{M}=\frac{\Delta L-\dot{M}_-\Delta(H+\phi)}{H_+ +f\Delta\phi}$$

where, for the jth bin from the centre,

$$f=\frac{\frac{1}{2}j^2-\frac{2}{3}j+\frac{1}{4}}{j^2-j+\frac{1}{3}}.$$

Once the densities and temperatures have been obtained these formulae can be applied from the centre outwards to produce a mass flow profile [Fig. 9(b)]. The resulting mass-flow rate rises from $0.1\,M_\odot\,\mathrm{yr}^{-1}$ at 1 kpc to $\simeq 0.7\,M_\odot\,\mathrm{yr}^{-1}$ at around 50 kpc where the cooling time becomes of order a Hubble time. This is in agreement with our deductions above.

5 Discussion

X-ray observations of elliptical galaxies show that a large fraction of them contain substantial quantities of hot gas. This gas is part of a cooling flow which is almost hydrostatic in the outer regions. In the case of NGC 4472 the gas cannot be contained by the visible matter and so, following FJT, we postulate a dark halo of non-luminous matter to provide a suitable potential well. The best-fit halo has the form

$$\varrho_{\mathrm{dark}}=\frac{0.028\pm0.006}{1+(r/10\,\mathrm{kpc})^2}\,T_7\,M_\odot\,\mathrm{pc}^{-3},$$

corresponding to a mass distribution of

$$M_{\mathrm{dark}}=(3.5\pm0.8)\,T_7\times10^{10}\,M_\odot\,\mathrm{kpc}^{-1}.$$

This will obviously be modified if the distance we have used is incorrect but the form of the solution will be the same. If we put distance $D\rightarrow D\times\theta$ we have

$\sigma\rightarrow\sigma$, and so from stellar hydrodynamics $\varrho_* a^2\rightarrow\varrho_* a^2$,

$a\rightarrow a\theta$, therefore $\varrho_*\rightarrow\varrho_*\theta^{-2}$; $M_*\rightarrow M_*\theta$,

$L\rightarrow L\theta^2$ giving $\alpha\rightarrow\alpha\theta^{-1}$.

Then puting $T\rightarrow T$, $n\rightarrow n\theta^{-1/2}$ and $u\rightarrow u\theta^{1/2}$ leaves all the dimensionless constants in equations (1), (2) and (3) unchanged.

The gas is in hydrostatic equilibrium throughout the galaxy and so the gas cooling in the inner regions is being supplied either by the outer regions of the galaxy or from an external source. We have argued in Section 3.3 that much of the gas lost by stars does not enter the flow, but that it is more likely to do so in the outer regions. Even if up to half the stellar mass loss does enter the

flow, however, the amount of mass supplied is too little to produce the steady-state flow rate of the model outside 16 kpc. One note of caution is that in the outer regions (≃50 kpc) the cooling time is comparable to the age of the system and the steady-state model may not adequately describe the system there. In spite of this it seems likely that at least some of the gas in the flow comes from outside the galaxy.

The most obvious explanation for the origin of the gas found in clusters is that it is lost from member galaxies during formation, and possibly via winds or tidal stripping since. If NGC 4472 is really at the centre of a loose group, then the same mechanism may apply and the outer part of the flow may come from an intragroup medium. Another possibility is that increased activity of the active galactic nucleus in the past has heated the gas and expelled it from the galaxy, and that it is now cooling and falling back in. Whatever the source of gas in NGC 4472 the correlation $L_x \propto L_0^{1.5-2}$ (Nulsen *et al.* 1984; Trinchieri & Fabbiano 1985) does suggest that stellar mass loss is responsible for $\dot{M}$ in most elliptical galaxies whose gas content and mass flow rates would otherwise be heavily dependent on their environment.

The preceding discussion suggests that approximately $\frac{1}{2} M_\odot$ of gas is deposited within the galaxy per year – in addition to that from stellar mass loss. Over a Hubble time this gives $10^{10} M_\odot$. This amount of material cannot be present as cool gas since it would be detected in 21-cm or optical-emission lines. The deposited material is thus most likely forming stars – at a rate similar to that in spirals! *IUE* observations show an ultraviolet excess below 2200 Å which may indicate a population of young main-sequence OB stars (the other possibility is that this excess comes from horizontal branch stars, Oke, Bertola & Capaccioli 1981). Hα filaments of the type seen in clusters have not been found in NGC 4472 (Kennicutt & Kent 1983; van den Bergh & Pritchett 1985), although given the relatively low mass-flow rate this is not surprising. Spectra of these filaments in other galaxies, e.g. NGC 1275, are inconsistent with the predicted star formation rates for an initial mass function as observed locally (Fabian, Nulsen & Arnaud 1984). However, the physical conditions in cooling flows considerably lower the Jeans mass and the initial mass function may be completely different (Fabian *et al.* 1982; Sarazin & O'Connell 1983). The required star formation rate in NGC 4472 is so low that we cannot comment on this. If stellar mass loss is important then the flow will carry processed material to the centre, leading to the formation of metallicity and perhaps colour gradients.

The lifetime against sputtering of dust grains in a 10^7 K gas is approximately $2\times10^4 n_H^{-1} a_{-6}$ yr where the grain size is $a_6\times10^{-6}$ cm (Draine & Salpeter 1979). The ratio of this to the cooling time is $10^{-3} a_{-6} T_7^{-1.6}$, so the majority of the dust is destroyed at its point of injection into the hot gas. Nevertheless, dust which is produced by stellar mass loss and does not join the hot phase may be preserved. Some of this gas may be carried into the centre and help to explain dust lanes and other features which appear to be common in elliptical galaxies.

Some of the gas in the cooling flow will reach the central regions of the galaxy where rotation and non-sphericity become important. Enough gas may be supplied to power an active nucleus, and the pressure of the hot gas and of magnetic fields dragged in by the flow may help to confine radio jets.

Finally it is worth stressing that in reality there are probably many gas phases with different densities, temperatures and metallicities. Our model is an attempt to describe the average behaviour of the system.

Acknowledgments

I thank Drs W. Forman and C. Jones for acquiring and reducing the X-ray data used in this paper, and Professor A. C. Fabian for many helpful suggestions and useful discussions. I acknowledge a SERC postgraduate studentship.

References

Bertola, F., Capaccioli, M., Holm, A. V. & Oke, J., B., 1980. *Astrophys. J.*, **237,** L65.
Biermann, P. & Kronberg, P., 1983. *Astrophys. J.*, **268,** L69.
Birkinshaw, M. & Davies, R. L., 1985. *Astrophys. J.*, **291,** 32.
Cowie, L. L., Fabian, A. C. & Nulsen, P. E. J., 1980. *Mon. Not. R. astr. Soc.*, **191,** 399.
Davies, R. L., 1981. *Mon. Not. R. astr. Soc.*, **194,** 879.
Davies, R. L., Efstathiou, G., Fall, S. M., Illingworth, G. & Schechter, P. L., 1983. *Astrophys. J.*, **266,** 41.
Draine, B. T. & Salpeter, E. E., 1979. *Astrophys. J.*, **231,** 77.
Efstathiou, G., Ellis, R. S. & Carter, D., 1980. *Mon. Not. R. astr. Soc.*, **193,** 931.
Ekers, R. D. & Kotanyi, C. G., 1978. *Astr. Astrophys.*, **67,** 47.
Fabbiano, G., 1985. Preprint.
Faber, S. M. & Gallagher, J. S., 1976. *Astrophys. J.*, **204,** 365.
Fabian, A. C., Hu, E. M., Cowie, L. L. & Grindlay, J., 1981. *Astrophys. J.*, **248,** 47.
Fabian, A. C., Nulsen, P. E. J. & Arnaud, K. A., 1984. *Mon. Not. R. astr. Soc.*, **208,** 179.
Fabian, A. C., Nulsen, P. E. J. & Canizares, C. R., 1982. *Mon. Not. R. astr. Soc.*, **201,** 933.
Feigelson, E. D., Schreier, E. J., Delvaille, J. P., Giacconi, R., Grindlay, J. E. & Lightman, A. P., 1981. *Astrophys. J.*, **251,** 31.
Forman, W., Jones, C. & Tucker, W., 1985. *Astrophys. J.*, **293,** 102.
Forman, W., Schwarz, J., Jones, C., Liller, W. & Fabian, A. C., 1979. *Astrophys. J.*, **234,** L27.
Huchra, J. P., Davis, R. J. & Latham, D. W., 1984. In: *Clusters and Groups of Galaxies,* p. 79, eds Mardirossian, F., Giuricin, G. & Mezzetti, M., Reidel, Dordrecht, Holland.
Huchtmeier, W. K., Tammann, G. A. & Wendker, H. K., 1975. *Astr. Astrophys.*, **42,** 205.
Kennicutt, R. C. & Kent, S. M., 1983. *Astr. J.*, **88,** 1096.
King, I. R., 1966. *Astr. J.*, **71,** 64.
King, I. R., 1978. *Astrophys. J.*, **222,** 1.
Kumar, C. K. & Thonnard, N., 1983. *Astr. J.*, **88,** 260.
Lauer, T. R., 1985. *Astrophys. J.*, **292,** 104.
Long, K. S. & van Speybroeck, L., 1983. In: *Accretion Driven Stellar X-ray Sources,* p. 117, eds Lewin, W. H. G. & van den Heuvel, E. P. J., Cambridge University Press.
Mathews, W. G. & Baker, J. C., 1971. *Astrophys. J.*, **170,** 241.
Nulsen, P. E. J., 1982. *Mon. Not. R. astr. Soc.*, **198,** 1007.
Nulsen, P. E. J., 1985. Preprint.
Nulsen, P. E. J., Stewart, G. C. & Fabian, A. C., 1984. *Mon. Not. R. astr. Soc.*, **208,** 185.
Oke, J. B., Bertola, F. & Capaccioli, M., 1981. *Astrophys. J.*, **243,** 453.
Osterbrock, D. E., 1960. *Astrophys. J.*, **132,** 325.
Raymond, J. C., Cox, D. P. & Smith, B. W., 1976. *Astrophys. J.*, **204,** 290.
Raymond, J. C. & Smith, B. W., 1977. *Astrophys. J. Suppl.*, **35,** 419.
Sandage, A., Binggeli, B. & Tammann, G. A., 1984. In: *Proc. of the ESO Workshop on the Virgo Cluster,* p. 239, eds Richter, O. G. & Binggeli, B.
Sarazin, C., L. & O'Connell, R. W., 1983. *Astrophys. J.*, **268,** 552.
Stewart, G. C., Canizares, C. R., Fabian, A. C. & Nulsen, P. E. J., 1984. *Astrophys. J.*, **278,** 536.
Tammann, G. A., 1974. In: *Supernovae and Supernova Remnants,* p. 155, ed. Cosmovici, C. B., Reidel, Dordrecht, Holland.
Tanaka, K. I., 1985. *Publs astr. Soc. Japan,* **37,** 133.
Trinchieri, G., 1985. Preprint.
Trinchieri, G. & Fabbiano, G., 1985. *Astrophys. J.*, **296,** 447.
van den Bergh, S. & Pritchett, C. J., 1985. Preprint.
White, R. E. & Chevalier, R. A., 1983. *Astrophys. J.*, **275,** 69.
White, R. E. & Chevalier, R. A., 1984. *Astrophys. J.*, **280,** 561.